

Drift wave transport scalings introduced by varying correlation length

J. Weiland and I. Holod

Department of Electromagnetics, Chalmers University of Technology and EURATOM-VR Association, 41296 Göteborg, Sweden

(Received 13 September 2004; accepted 11 October 2004; published online 14 December 2004)

Scalings of the correlation length of drift wave turbulence with magnetic current q , shear, elongation, and temperature ratio have been introduced into a drift wave transport model. The correlation length is calculated from linear scaling of the fastest growing mode. Such a procedure is supported by previous turbulence simulations with absorbing boundaries for short and long wavelengths. The resulting q and s scalings are now in better agreement with experimental scalings. In particular, the simulation results for transport barrier shots improve. © 2005 American Institute of Physics. [DOI: 10.1063/1.1828083]

I. INTRODUCTION

Although drift wave models have been rather successful in describing tokamak transport, some types of scalings, mainly for geometrical parameters, are still not fully understood. One of these is current q scaling and another is the dependence of transport on magnetic shear. The last dependence is particularly important for the formation of transport barriers. A general trend is that electrostatic modes are less sensitive to the magnetic field geometry than electromagnetic modes. Because of this many electrostatic models have had problems to recover effects of magnetic geometry. With increasing beta, however, also electromagnetic drift wave models become more sensitive to geometry. Another aspect is that eigenvalue problems have often been solved in the strong ballooning limit where the effect of averaging the driving term from magnetic field curvature vanishes. This has, however, turned out to be insufficient for the model we will consider here. The natural next step is then to consider nonlinear effects. The general nonlinear case is, of course, extremely complicated. In a typical magnetic fusion plasma, however, we can assume a state with stationary turbulence, i.e., where the external conditions and heating are varying on much longer time scales than that needed to obtain a stationary turbulent spectrum. Even in this case the situation can be rather complicated with several unstable modes peaking at different space scales. The boundary conditions in k space are also going to play important roles. Concerning ion temperature gradient (ITG) modes, and to some extent trapped electron (TE) modes, however, we now have sufficient experience from turbulence simulations to make reasonable assumptions about the nonlinear correlation length. Our first simulations^{1,2} were made in the local limit with viscosity and artificial damping for long wavelengths corresponding to absorbing boundaries for both short and long wavelengths. The transport was well described by a quasilinear formula including only one mode number, corresponding to the inverse correlation length. This mode number was close to that of the linearly fastest growing mode. We have recently recovered the same transport level in simulations where the artificial low k damping is replaced by zonal flows, self-consistently generated by the turbulence.³ This required a sufficiently

large radial box size. This confirms the possibility to use one correlation length for the transport due to ITG modes to more realistic simulations. This fact can be understood from the fact that the fastest growing mode represents the source of the turbulence and with absorbing boundaries in k space: it is natural that the source will define the correlation length.⁴ The situation becomes more complicated when we have more than one instability. However, we have also included the TE mode in simulations with local geometry.² These simulations gave good results both for χ_i and χ_e when we used the ITG correlation length. In this system the isolated TE mode is not dispersive so it is probably the coupling to the ITG mode that gives the common correlation length.

In the more realistic geometry used in Refs. 5 and 6, the location of the linearly fastest growing mode in k_y depends on geometry variables and on the temperature ratio T_e/T_i .

In the present work we have obtained a scaling of the fastest growing mode with several variables by running a linear numerical code. We have then used this mode for the correlation length in the quasilinear transport coefficients for a drift wave transport model. We then study scalings of transport coefficients in different parameter regimes and also make a predictive simulation of a transport barrier shot on Joint European Torus (JET).⁷

II. FORMULATION

The drift wave model has been described in several papers and in a book.⁸ We use the usual low frequency drifts and make a fluid closure assuming that the heat flux equals the Braginskii diamagnetic heat flow, i.e.,

$$\frac{3}{2}n_i\left(\frac{\partial}{\partial t} + \mathbf{v} \cdot \nabla\right)T_i + P \nabla \cdot \mathbf{v} = -\nabla \mathbf{q}_*, \quad (1a)$$

where

$$\mathbf{q}_* = \frac{5}{2} \frac{P}{m\Omega_c} (\hat{e}_{\parallel} \times \nabla T). \quad (1b)$$

This leads to the temperature perturbation,

$$\frac{\delta T_i}{T_i} = \frac{1}{\omega - (5/3)\omega_{Di}} \left[\frac{2}{3} \omega \frac{\delta n_i}{n_i} + \left(\eta_i - \frac{2}{3} \right) \omega_{*e} \right] \frac{e\phi}{T_e}. \quad (2)$$

In the simplest case with Boltzmann electrons, quasilinearity leads to a further simplification of Eq. (2). The eigenvalue equation, using the ballooning mode formalism,⁹ can be written in the form^{6,10}

$$\frac{\partial^2 \phi}{\partial \theta^2} + [(B + C(\Omega)k_{\perp}^2 \rho_s^2)A(\theta) + \varepsilon_n g(\theta)]\phi = 0, \quad (3)$$

where $k_{\perp}^2 = k_{\theta}^2(1 + \hat{s}^2 \theta^2)$ and

$$g(\theta) = \cos(\theta) + s\theta \sin(\theta),$$

where $s = (r/q)(dq/dr)$, q is the safety factor, θ is the generalized poloidal angle in the ballooning formalism and¹¹

$$\hat{s} = \sqrt{2s - 1 + \kappa^2(s - 1)^2},$$

where κ is the elongation.

The definitions of A and B are given in Ref. 6.

This eigenvalue problem can be solved approximately analytically by using a quadratic form and the asymptotic eigenfunction as trial function.^{6,10} The asymptotic eigenfunction is

$$\hat{\phi} \sim e^{-\alpha \theta^2}, \quad (4a)$$

where

$$\alpha = -i\tilde{\omega}k_{\theta}^2 \rho_s^2 \hat{s}q. \quad (4b)$$

Here $\tilde{\omega} = \omega/\omega_{De}$, and α was simplified by omitting a phase factor given in Ref. 6.

The nonlocal effects are basically the magnetic shear damping described by

$$\gamma_s = \frac{\hat{s}}{q} \omega_{De}, \quad (5)$$

and the averaging of the driving curvature term over the mode profile described by

$$\langle g \rangle = \frac{\int g(\theta) |\phi|^2 d\theta}{\int |\phi|^2 d\theta}. \quad (6)$$

The average $\langle g \rangle$ depends sensitively on the width of the eigenfunction with smaller values for wider eigenfunctions. Thus we can see directly from Eq. (4b) that a small \hat{s} will require a large k_{θ} in order to maintain a finite $\langle g \rangle$, i.e., a finite instability drive. Thus we expect a shorter correlation length for a smaller \hat{s} . This usually has a stronger effect in reducing transport than the direct effect of a small s in $g(\theta)$. In a similar way an increased current reduces q and thereby increases the mode width; thus a more favorable current scaling is expected.

Although we should expect the correlation length to coincide with the wavelength of the linearly fastest growing mode, this is clearly a rather rough argument. We know that higher mode number is more strongly damped by diffusion. In fact the correlation length seen in simulations more typically coincides with that of the fastest growing mode when the growth rate is normalized by the drift frequency. This value often corresponds to $k_{\theta}^2 \rho_s^2 = 0.1$. This value is only

weakly dependent on the temperature gradient. A very interesting observation is that a quasilinear diffusion coefficient with only one mode number has been able to reproduce scalings of χ_i with η_i almost perfectly in turbulence simulations.^{1,5,13} This scaling is almost linear in a large regime of η_i . Since the linear growth rate can be written as

$$\gamma = \omega_{*e} \sqrt{\frac{\varepsilon_n}{\tau} (\eta_i - \eta_{i\text{th}})}, \quad (7)$$

this indicates a scaling

$$\chi_i \sim \gamma^2 / k_x^2 \omega_{*e}. \quad (8)$$

The scaling $\chi_i \sim \eta_i - \eta_{i\text{th}}$ following from Eqs. (7) and (8) has been found both in our own turbulence simulations^{1,2} and in simulations by Hamaguchi and Horton.¹³ This scaling has also been derived from our diffusion coefficient,^{1,14,15}

$$\chi_i = \frac{1}{\eta_i} \left(\eta_i - \frac{2}{3} - \frac{10}{9\tau} \right) \frac{\gamma^2 / k_x^2}{(\omega_r - (5/3)\omega_{Di})^2 + \gamma^2} \quad (9)$$

in a region from 1.1 $\eta_{i\text{th}}$ to roughly 2 $\eta_{i\text{th}}$ by using the linear dispersion relation. However, the deviation from this scaling increases slowly above 2 $\eta_{i\text{th}}$. Thus the ω_r dependence (non-Markovian effect) of χ_i is important. We have determined the maximum of γ/ω_{*e} as a function of $k_{\theta} \rho_s$ by running a linear code which used averages over the eigenfunction Eq. (4a) for nonlocal quantities.

The turbulence simulations mentioned in the Introduction all used $T_e = T_i$. A generalization to $T_i \neq T_e$ introduces a difference between the polarization drift and the finite Larmor radius (FLR) drift which enters directly into the usual Gyro-Bohm condition which previously has meant $k_{\theta} \rho_s$ where $\rho_s = c_s / \Omega_{ci}$ and $c_s = \sqrt{T_e/m_i}$.

Numerical tests have indicated that the usual simple drift wave dependence remains. This means that we can replace T_e by $\frac{1}{2}(T_e + T_i)$ in the correlation length scaling.

The overall numerical scalings have resulted in the following numerical fit for the correlation length:

$$\text{FLS} = \left(0.7 + \frac{2.4}{7.14q\hat{s} + 0.1} \right) \text{FL}, \quad (10a)$$

$$k_{\theta} \rho_s = \sqrt{\frac{2\text{FLS}}{1 + (1/\tau)}}, \quad (10b)$$

where FL is the FLR parameter presently used, i.e., 0.1.

III. RESULTS

Scalings with magnetic shear s , magnetic q , and temperature ratio τ for new and old models are shown in Figs. 1–3. Here we used cyclone parameters.

The new model gives lower transport level in the region of negative magnetic shear, $s < -0.4$ (Fig. 1). The difference between old and new model in τ and q scalings (Figs. 2 and 3) is not very strong for the Cyclone base case parameters, however, the new model gives a stronger dependence on q which is in the direction giving a more favorable current scaling of confinement.

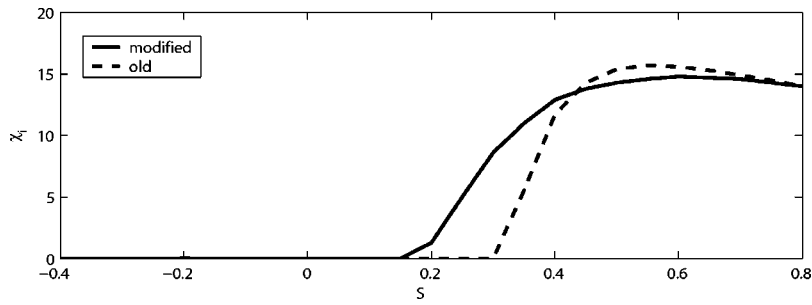


FIG. 1. Scaling of transport with magnetic shear using data from Ref. 12.

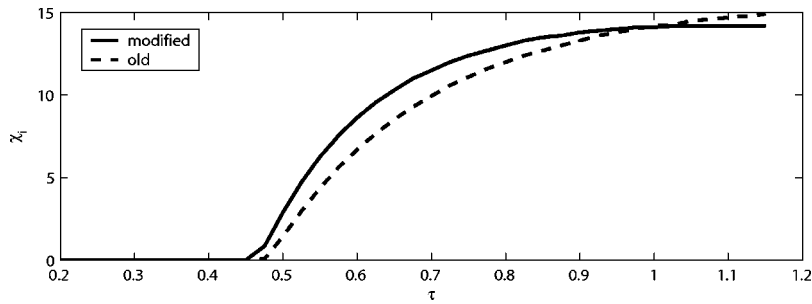


FIG. 2. Scaling of transport with temperature ratio using data from Ref. 12.

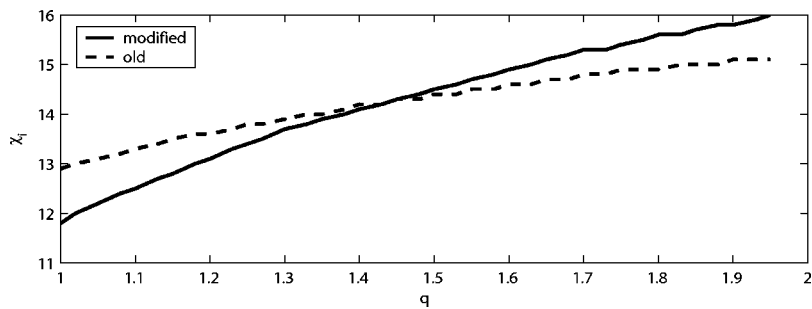


FIG. 3. Scaling of transport with safety factor using data from Ref. 12.

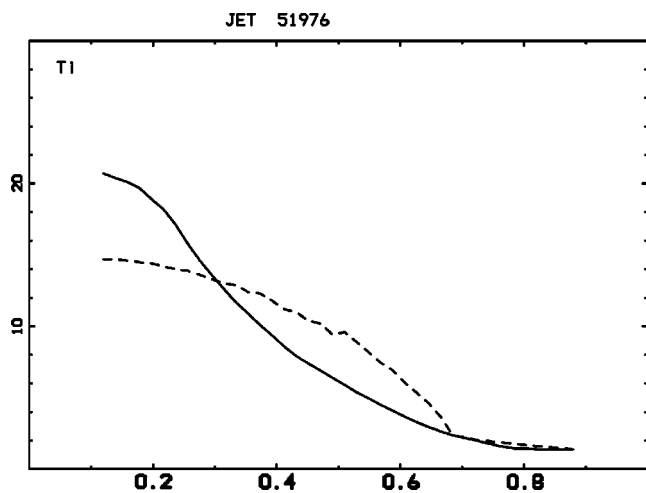


FIG. 4. Predictive simulation of JET 51976 using fixed correlation length. The solid line is the experimental temperature and the dashed line is the simulation.

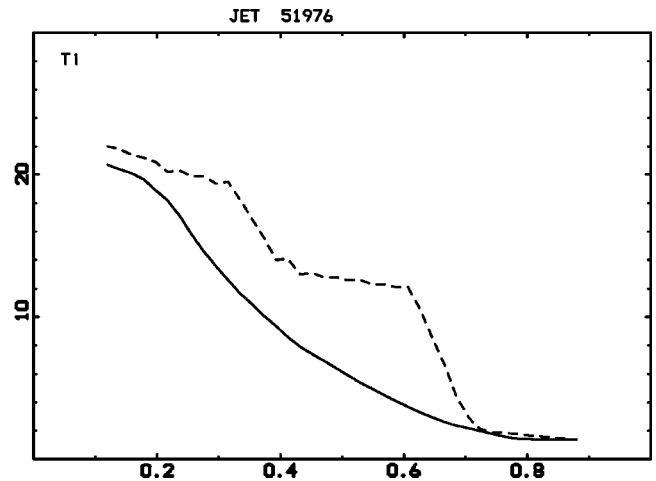


FIG. 5. Predictive simulation of JET 51976 using our modified model with correlation length given by Eq. (10). The solid line is the experimental temperature and the dashed line is the simulation. The experiment developed an edge transport barrier shortly after the time of the simulation.

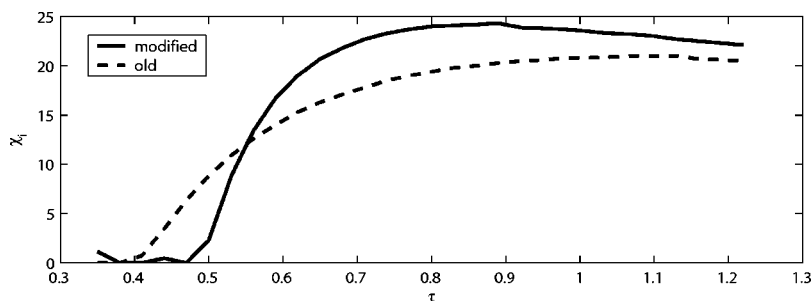


FIG. 6. Scaling of transport with temperature ratio using data from JET 51976 at an interior point.

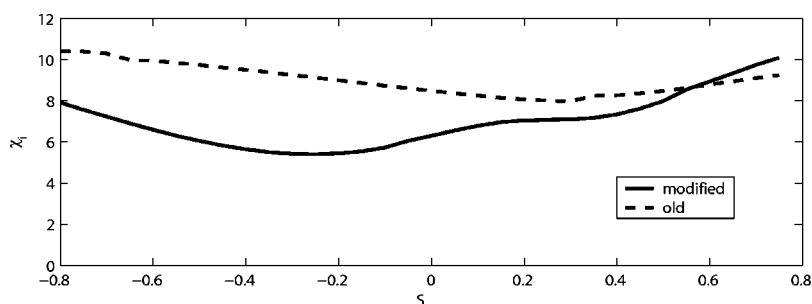


FIG. 7. Scaling of transport with magnetic shear using data from JET 51978 at an interior point.

As the result of the increased shear dependence we also show simulations of JET 51976 (Ref. 16) with both the old and the new model (Figs. 4 and 5). The new code gives a strong transport barrier close to the edge (Fig. 5) which is not in the experiment at this time, however, such a barrier developed shortly after. The system is clearly very sensitive in this regime. However, the difference between old and new model is well established.

The τ scaling for JET 51976 parameters is shown in Fig. 6. As we can see the new model gives significantly lower transport for $\tau < 0.55$, which was the situation in the interior parts of the discharge.

We also present the s scaling for parameters similar to JET 51976 (Fig. 7). We use smaller elongation $\kappa=1.2$ which can be justified close to the axis. We can see the pronounced difference between old and new model, with more favorable effect of small magnetic shear in the new model.

IV. CONCLUSIONS

We have presented a drift wave transport model which uses a single scale length (correlation length) which, however, depends on plasma and geometry parameters such as temperature ratio, magnetic shear, magnetic q , etc. The result is an improvement over a model using a fixed scale length. The main improvement is in the description of transport barriers. However, also general scalings, such as current scaling, are improved. Of course using only one scale length reduces the computing time considerably as compared to models using many scale lengths. At the same time, using a formula

like Eq. (10) for the correlation length leads to increased physics insight.

One important observation from Ref. 6 which also shows in the present scalings is that elongation reduces the beneficial effects of small magnetic shear. The present extension of the model can, in some cases, partly restore the effect of magnetic shear.

¹J. Weiland and H. Nordman, Proceeding of the Varenna–Lausanne International Workshop, Theory of Fusion Plasmas, Chexbres, 1988, p. 451; H. Nordman and J. Weiland, Nucl. Fusion **29**, 251 (1989).

²H. Nordman, J. Weiland, and A. Jarmen, Nucl. Fusion **30**, 983 (1990).

³We here used a Connor–Taylor equilibrium.

⁴It is important to realize that although longer wavelengths in themselves would give larger transport, these larger eddies will be torn apart by shorter eddies in such a way that the effective scale length for transport will be the correlation length.

⁵S. Dastgeer, S. Mahajan, and J. Weiland, Phys. Plasmas **9**, 4911 (2002).

⁶J. Weiland, Phys. Plasmas **11**, 3238 (2004).

⁷P. H. Rebut, R. J. Bickerton, and B. E. Keen, Nucl. Fusion **25**, 1011 (1985).

⁸J. Weiland, *Collective Modes in Inhomogeneous Plasmas, Kinetic and Advanced Fluid Theory* (IOP, Bristol, 2000).

⁹J. W. Connor, R. J. Hastie, and J. B. Taylor, Phys. Rev. Lett. **40**, 396 (1978).

¹⁰S. C. Guo and J. Weiland, Nucl. Fusion **37**, 1095 (1997).

¹¹D. D. Hua, X. Q. Xu, and T. K. Fowler, Phys. Fluids B **4**, 3216 (1992).

¹²A. M. Dimits, G. Bateman, M. A. Beer *et al.*, Phys. Plasmas **7**, 969 (2000).

¹³S. Hamaguchi and W. Horton, Phys. Fluids B **2**, 3040 (1990).

¹⁴A. Zagorodny and J. Weiland, Phys. Plasmas **6**, 2359 (1999).

¹⁵A. Heikkilä and J. Weiland, Phys. Fluids B **5**, 2043 (1993).

¹⁶C. D. Challis, X. Litaudon, G. Tresset *et al.*, Plasma Phys. Controlled Fusion **44**, 1031 (2002).